Ann Ist Super Sanità 2012 | Vol. 48, No. 1: 10-18
DOI: 10.4415/ANN_12_01_03

Role of X-ray microtomography in tissue engineering

Andrea Barbetta[(a)], Rossella Bedini[(b)], Raffaella Pecci[(b)] and Mariella Dentini[(a)]
[(a)] *Dipartimento di Chimica, Sapienza Università di Roma, Rome, Italy*
[(b)] *Dipartimento di Tecnologie e Salute, Istituto Superiore di Sanità, Rome, Italy*

Summary. The structure and architecture of scaffolds are crucial factors in scaffolds-based tissue engineering since they affect the functionality of the tissue engineering construct and the eventual application in health care. Therefore, effective scaffold assessment techniques are required right at the initial stages of research and development so as to select or design scaffolds with suitable properties. Furthermore, since the biological performances of a scaffold is evaluated with respect to its capacity of favouring cell adhesion, proliferation as well as production of extracellular matrix, it is important to have an analytical technique able to monitor the various stages of cell culture both *in vitro* and especially *in vivo*. Finally, the development of a vascular network inside the cell scaffold construct is a fundamental requisite for achieving a full integration of the developing tissue with the host tissue. Also in this respect it is mandatory to assess the propensity of the scaffold to be permeated by blood vessels. In the review, it will be shown how X-ray microtomography (micro-CT) can give fundamental information regarding all the three aspects outlined above.

Key words: X-ray microtomography, tissue engineering, scaffolds, vascularization, tissue-engineered bone.

Riassunto *(Il ruolo della microtomografia nella ingegneria dei tessuti)*. La struttura e l'architettura degli *scaffold* sono fattori importantissimi nell'ingegneria dei tessuti poiché influenzano la funzionalità dei tessuti ricostruiti e una loro eventuale applicazione in campo sanitario. È necessaria infatti, nelle prime fasi della ricerca, una valutazione tecnica degli *scaffold* in modo da selezionare o progettare quelli con proprietà più adeguate. Inoltre, poiché le prestazioni biologiche di uno *scaffold* sono valutate rispetto alla capacità di favorire l'adesione e la proliferazione delle cellule seminate e contemporaneamente la produzione di una matrice extra-cellulare, è molto importante ricorrere all'uso di una tecnica analitica che sia in grado di monitorare le varie fasi della coltura cellulare, sia *in vitro* che *in vivo*. In ultimo, lo sviluppo di una rete vascolare all'interno della proliferazione cellulare dello *scaffold* è uno dei requisiti fondamentali per permettere la completa integrazione del tessuto in fase di sviluppo con il tessuto ospite. Anche in questo caso è assolutamente necessario valutare la propensione dello *scaffold* alla permeazione da parte di vasi sanguigni. In questa rassegna, sarà mostrato come la microtomografia a raggi X (micro-CT) sia in grado di fornire importanti informazioni riguardo ai tre aspetti evidenziati poco sopra.

Parole chiave: microtomografia a raggi X, ingegneria tissutale, *scaffold*s, vascolarizzazione, tessuto osseo ingegnerizzato.

INTRODUCTION

A frontier research discipline of nowadays is represented by tissue engineering, a multidisciplinary approach to the problem of restoring diseased or damaged tissues to its original state and function.

The innovative concept underlying tissue engineering with respect to the traditional methods of regenerative medicine (*i.e.* the employment of prostheses and organ transplantation) is the use of autologous cells, obtained from a biopsy of the patient. Three common strategies employed in tissue regeneration are:

1. infusion of isolated cells;
2. cells are included in a gel precursor solution which is injected in the site requiring restoration and subsequently cured *in situ*;
3. implantation of a cell-scaffold composite. Cells are seeded on a porous scaffold which has the role of supporting and guiding cells towards the development of tissue-like structures as well as providing a platform for the delivery under controlled release condition of growth, angiogenic factors, etc.

Of the three strategies, the use of cell-scaffold composites generally leads to a more successful outcome. These scaffolds are often critical, both *in vitro* as well as *in vivo*, to recapitulating the normal tissue development process and allowing cells to formulate their own microenvironments. In contrast to using cells alone, a scaffold provides a 3D matrix on which the cells can proliferate and migrate, produce matrix, and form a functional tissue with a desired shape. The scaffold

Address for correspondence: Andrea Barbetta, Dipartimento di Chimica, Sapienza Università di Roma, Piazzale Aldo Moro 5, 00185 Rome, Italy. E-mail: andrea.barbetta@uniroma1.it.

also provides structural stability for developing tissue and allows incorporation of biological or mechanical signals to enhance tissue formation. The biological and mechanical properties of scaffolds may vary depending on the application, and can be designed to provide an environment with appropriate signals that stimulate cells to proliferate and/or differentiate.

The design or selection of porous scaffolds for specific tissue engineering applications requires an understanding of the relationship between the scaffold micro architecture and its intended biological and mechanical functions. Biological responses to implanted scaffolds are influenced by a wide variety of factors including scaffold design features such as material, degradation rate, and 3D micro architecture [1, 2]. For instance, one of the key properties that is widely discussed in the literature is porosity [3, 4]. Porosity would determine cell seeding efficiency, diffusion and the mechanical strength of the scaffold. High porosity and high surface area to volume ratio are required for uniform cell delivery, cellular attachment and neo tissue ingrowths' [5, 6].

Studies on scaffold design have revealed that besides porosity, other factors such as pore interconnectivity and permeability affect cell migration, fluid exchange and eventually tissue ingrowth and vascularization (penetration of blood vessels). Other parameters which are used to assess the functionality of the scaffold would include surface area and pore size. A large surface to volume ratio would assist cellular adhesion. Moreover, pore sizes should be sufficiently large so as to encourage cellular ingrowth. Depending on the tissue type (soft or hard tissue), some of the tissue engineered construct must posses sufficient mechanical strength so as to withstand loading, thus strut/wall thickness, anisotropy and the cross sectional area of the scaffold would be of interest.

The biological performances of a scaffold in terms of cell adhesion, proliferation and production of extracellular matrix is a factor that has to be evaluated during *in vitro* culturing and *in vivo* testing. Sometimes a combination of techniques is required so as to achieve an in depth study of the scaffold properties and of its performance. However, the most attractive option is a single technique which is non-destructive, yet capable of providing a comprehensive set of data. A recently developed technique which is non-destructive uses X-ray microtomography (micro-CT), which can produce 2D maps as well as 3D images of the porous scaffolds.

Micro-CT has been used to quantify complex geometries in 3D at small resolution. Images with voxel (the 3D equivalent of 2D pixel) sizes less than 10 μm are potentially achievable [7], making it superior to other techniques such as ultrasound (30 μm) and magnetic resonance imaging (100 μm). Micro-CT has predominantly been used for visualising and analysing bone structure and development [8] and to evaluate the 3D microarchitecture of subchondral trabecular bone in osteoarthritis [9].

In micro-CT scanning, the specimen is divided into a series of 2D slices which are irradiated from the edges with X-rays. Upon transversing through the slice, the X-rays are attenuated and the emergence X-rays with reduced intensities are captured by the detector array. From the detector measurements, the X-rays paths are calculated and the attenuation coefficients are derived. A 2D pixel map is created from these computations and each pixel is denoted by a threshold value which corresponds to the attenuation coefficient measured at a similar location within the specimen. As the attenuation coefficient correlates to the material density, the resultant 2D maps reveal the material phases within the specimen. The quality of the 2D maps is dependant on the scanning resolution which ranges from 1 to 50 μm [10-13]. At high resolution, intricate details are imaged, however more time is required for high resolution scanning and large processing and storage capabilities become necessary.

Scaffolds with intricate interior structures can be scrutinized using micro-CT, and any spatial location of the architecture can be digitally isolated out. This is crucial for scaffolds that exhibit different geometric layouts at different spatial locations. Within the digitally excised scaffold cube, scaffold material volume and surface area are measured, thus allowing the calculation of porosity and surface area to volume ratio. Three dimensional imaging allows a close up view of any specific location, thus the observation of pore shape and the measurement of pore size and strut/wall thickness can be conducted in these close ups. Scaffold anisotropy is evaluated via algorithms and the cross-sectional area can be measured from 2D slice images. By inverting the threshold, a negative image is created which captures only the scaffold pores. By measuring the total and the interconnected pore volumes, interconnectivity is derived [14]. As micro-CT employs penetrative X-rays, closed pores can be imaged. The flexibility of micro-CT analysis allows the evaluation of foams, textiles and nanofiber scaffold.

There are associated concerns despite of the numerous advantages of using micro-CT. Image thresholding is a crucial step that has to be executed prior to 3D modeling and it affects the subsequent analysis and visualization [15, 16]. In the conventional approach, the thresholding range is selected via histographics and visual estimation and the problem arises when the scaffold is composed of multiple materials whose thresholding ranges overlap and this renders the digital separation of these materials a difficult task. Moreover, as polychromatic X-ray beams are used in micro-CT, the lower energy rays would be readily attenuated by the sample resulting in a high exposure at the centre of the scaffold. This effect is known as beam hardening and as a result thresholding is no longer dependent solely on radiodensity but also on the specimen size [17, 18]. Micro-CT analysis is not suitable for scaffolds containing metals as X-rays are heavily

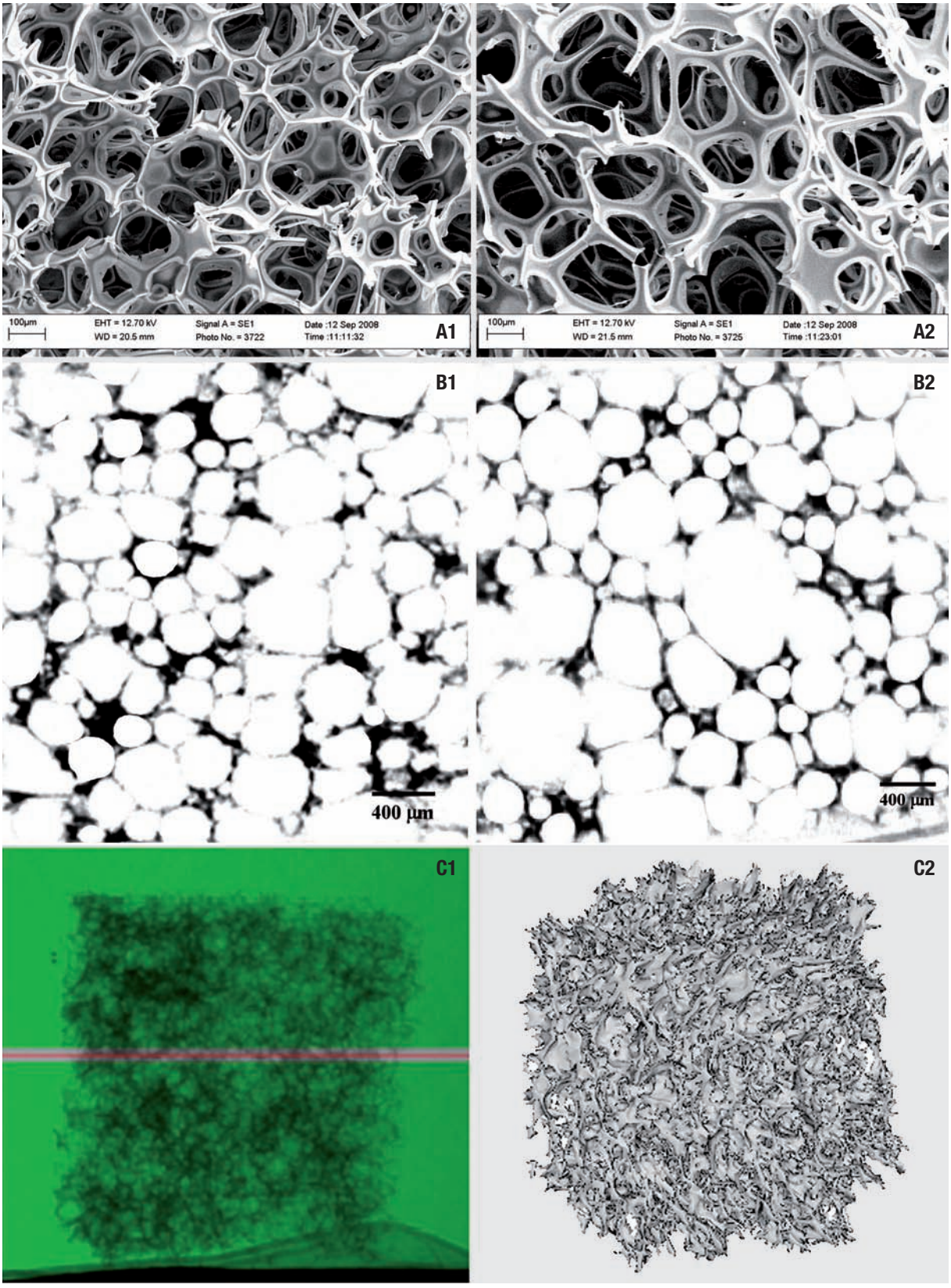

Fig. 1 | *(A) Scanning electron micrographs. (B) X-ray micro-tomography images of a solid foam 2D sections. (C1) Radiograph of the solid foam and (C2) 3D reconstruction of the entire scaffold.*
Nominal pore volumes (PV): 85% (A1 and B1) and 90% v/v (A2, B2, C1 and C2). Gelatin concentration: 12% w/v. Surfactant system used: poly-Quaternium (0.8% w/v) and SDS (0.08% w/v). Reproduced from Barbetta et al. *[24], with permission of The Royal Society of Chemistry.*

attenuated by these metals. The presence of metals results in dark and bright grainy artifacts which obscure important details in the scan images [19, 20]. As micro-CT is a relatively new technology, improved algorithms and setups are anticipated, thus resolving such imaging errors.

A micro-CT study

The potential of micro-CT scanning is demonstrated in the following application which involves the evaluation of the morphological characteristics of polymeric scaffolds that were produced via gas-in-liquid foam templating [21-23]. This method consists of insufflating under controlled condition a predetermined volume of an inert gas into a solution of a biopolymer and an appropriate surfactant and induce, in a successive step, the gelation of the film of liquid phase surrounding the bubbles of the gas phase. By dosing the volume of the gas insufflated, porous materials with very different pore volumes (from 75 to 95% v/v) can be readily synthesised. The ensuing porous materials are characterised by a trabecular morphology *(Figure 1 (A1) and (A2))*. In the present case two scaffolds made of gelatin and characterised by a nominal pore volume of 85 and 90% v/v were prepared. As already apparent from the SEM micrographs *(Figure 1 (A1) and (A2))*, the two samples although characterised by the same geometrical layout, are rather different in term of the size of voids (originated from the gas bubbles entrapped within the gelatin solution) and interconnects (hole openings in the void walls originated from the rupture of the film of continuous phase surrounding adjacent bubbles at the point of maximum approach). To visualize the scaffolds by micro-CT, it was necessary to stain them by a contrasting agent since the attenuation of the X-ray beam through the sample made of relatively light elements (C, N, O) and characterised by relatively low density is not enough to give rise to clear images. The specimens were soaked into a solution 1% w/v of osmium tetroxide. As it can been seen from the radiograph of *Figure 1 (C1)*, the contrast was satisfactory, the foam-like morphology of the specimen being well evident. As an example of the potentialities of micro-CT as a tool for monitoring the influence of the processing parameters on the final scaffold morphology, the representative 2D images of two scaffolds are reported in *Figure 1 (B1) and (B2)*. Already qualitatively, it is evident the pronounced effect exerted by the volume of gas insufflated on both the dimension of voids and interconnects. To assess the suitability of these scaffolds for the culture of different cell type it is important to obtain a quantitative measure of the void and interconnect diameter distributions. This information can be obtained from the elaboration of the 2D micrographs obtained with micro-CT *(Figure 1 (B1) and (B2))*. Void and interconnects size distributions for the two scaffolds are displayed in *Figure 2*. It is evident that both distributions shift to left side of the diameter axis

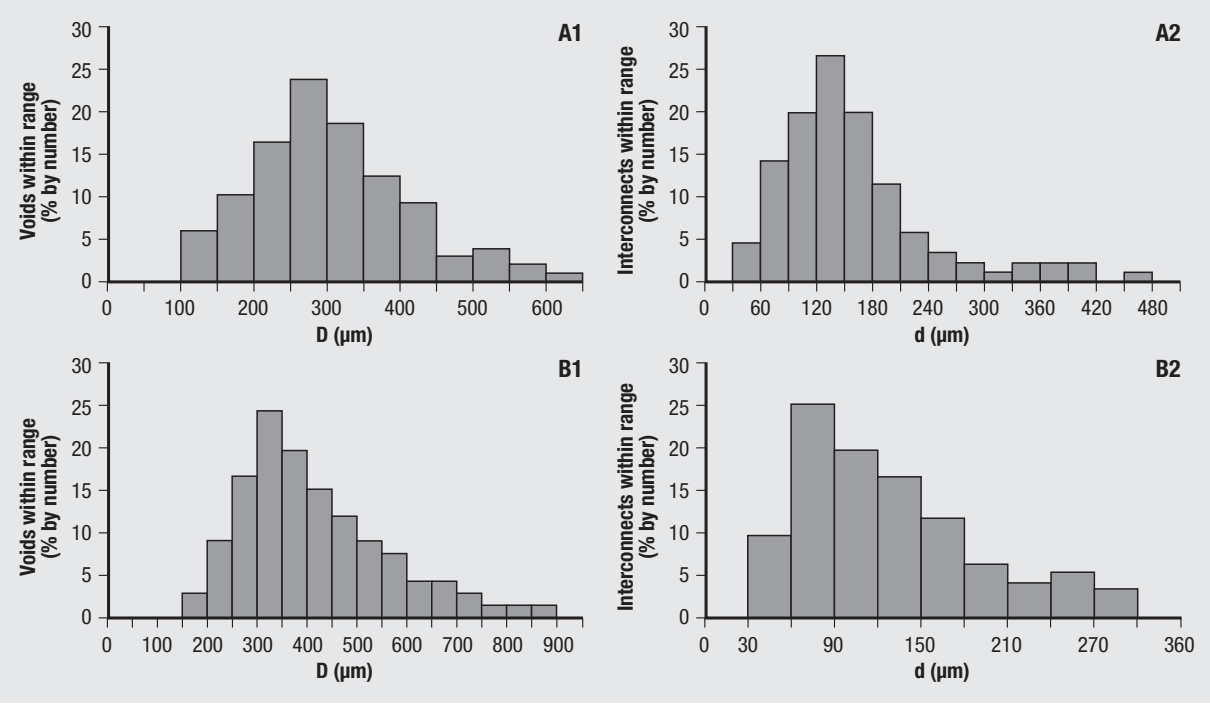

Fig. 2 | *Number-distributions of voids (1) and interconnects (2) size of gelatin (type B) solid foam characterised by a nominal pore volume (PV) of: (a) 85%; (b) 90% v/v. The area of a histogram bar is proportional to the number fraction of either voids or interconnects within a size range. Reproduced from Barbetta* et al. *[24], with permission of The Royal Society of Chemistry.*

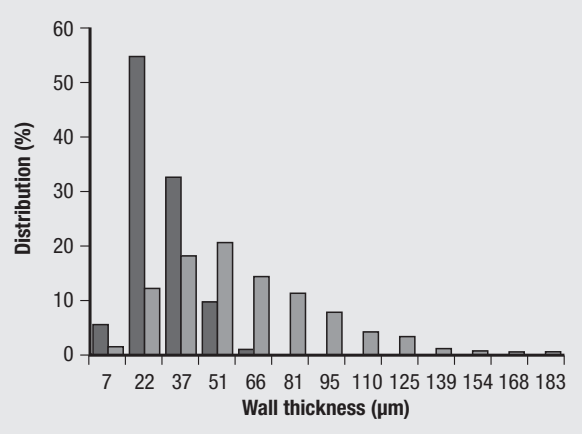

Fig. 3 | *Distribution of thicknesses computed from the 3D micro-CT images of the gelatin based scaffolds. Nominal pore volumes: red bars 85% v/v; blue bars 90% v/v.*

when the pore volume increases from 85 to 90 %v/v. *Table 1* reports the data regarding average void and interconnect diameters for the two scaffolds.

Quantitative parameters of the scaffolds structure such as porosity, surface area to volume ratio, average wall thickness and interconnectivity were then extracted. Quantification first requires to separate scaffold material from background. This is classically done by thresholding the image grey levels. The threshold was selected by analysing the histograms of the image which associate to each grey level, the number of voxels having this grey level. In this way for example, the distribution of scaffold wall thickness *(Figure 3)* can be obtained. *Table 1* reports the set of characterization data for the two scaffolds.

Hence this study demonstrates the versatility of micro-CT in evaluating scaffolds as it is a single technique which is capable of characterising the scaffolds in multiple aspects.

Study of the ex vivo *tissue engineering bone*

Ex vivo imaging of tissue-engineering constructs with micro-CT plays a critical role in the evolution of new formed bone and in the behaviour of scaffolds after implant. Traditional methods for evaluating osteointegration of tissue-engineered constructs are based on 2D techniques such as histology, scanning electron and fluorescence microscopy imaging. 3D structural data and 3D quantitative analysis of the newly formed bone within the scaffold are difficult to obtain by these techniques. Histological techniques involve the analysis of two-dimensional slices from tissue samples. Although, two dimensional slices can provide useful information concerning the nature of the new bone, the fibrous tissue and the blood marrow cells, at 2D level it becomes very difficult, if not impossible, the assessment of the scaffold and bone spatial structure. Moreover, it is practically impossible by histology techniques to obtain mean values of physical quantities such as the whole volume of the investigated sample. Finally, histology is a destructive method that does not allow further analysis of the samples. Conversely, radiography is a non-invasive method to obtain images throughout the time course of clinical experiments, but is suffering from the low image quality, due to a projection of a 3D structure on a plane thus making it difficult to attain accurate information. Unlike to the above methods, micro-CT employs conventional X-rays, which can achieve a resolution of about 10 µm, when commercial instruments are used, and up to 1 µm, when Synchrotron Radiation (SR) is used [24]. Based on the fact that new bone, fibrous tissue and ceramic scaffolds present different coefficients of absorption, this method permits to separate their 3D structures and to obtain the corresponding quantitative data such as bone volume, thickness, growth, destruction, remodeling and changes in bone density [25-27].

As an illustrative example, Mastrogiacomo demonstrated [28] the possibility of non-destructive, quantitative analysis of tissue engineering constructs to determine the total volume and thickness distribution of newly formed bone into implants in a small animal model by using the micro-CT technique. This methodology offers major advantages including the possibility of investigating the influence of scaffold parameters such as porosity and spatial distribution of walls with regard to the growth of bone within the implant. In a more recent work [29], taking advantage of micro-CT associated with SR, the kinetics of bone growth into tissue engineering constructs was investigated in an immunodeficient murine model. Images of the pure HA scaffolds were acquired before implantation and after 8, 16, and 24 weeks from implantation. In all cases, data were first obtained on the pure scaffold and then the same scaffold was seeded with cells, implanted and, after its recovery, analyzed again by micro-CT to investigate the kinetics of the new bone growth. After implantation in immuno-

Table 1 | *Nominal pore volume (PV), average void diameter (‹D›), average interconnect diameters (‹d›), degree of interconnection (‹d›/‹D›), experimental pore volume (PV_{exp}), interconnectivity and average wall thickness of gelatin solid foams*

PV[a] (% v/v)	‹D› (µm)	‹d› (µm)	‹d›/‹D›	PV_{exp}[b](% v/v)	Interconnectivity[c]	Average wall thickness (µm)
85	250 ± 20	80 ± 15	0.32	86 ± 3	100%	74 ± 5
90	360 ± 30	150 ± 20	0.41	89 ± 3	100%	38 ± 5

[a]Nominal Pore Volume corresponding to the volume of gas injected. [b]Experimental Pore Volume as determined from micro-CT. [c]defined as: 100% x volume of interconnected pores/volume sum of interconnected and closed pores.

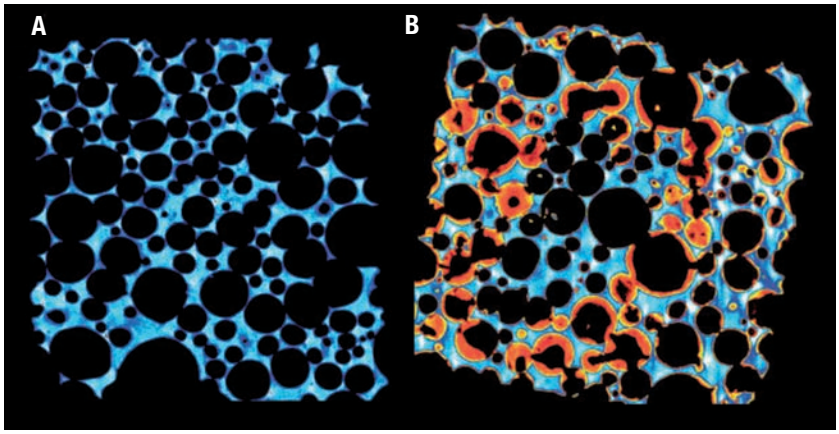

Fig. 4 | *Micro-CT analysis of the 100% HA scaffold before and after 4-months implantation. Panel A: a random segmented slice of the volume prior to cell seeding and implantation. Panel B: a random segmented slice of the volume after cell seeding and implantation for 4 months* in vivo. *Reproduced from Papadimitropoulos* et al. *[30], with permission of John Wiley and Sons.*

deficient mice, bone tissue formation was observed in the pores *(Figure 4)*. In addition, this newly formed bone was quantified at different time points following implantation. While in the case of the pre-implant scaffolds only one peak in the X-ray absorption histogram was observed corresponding to the biomaterial used for the manufacturing of the scaffold itself, in the case of the implanted samples an additional peak was observed at lower X-ray absorption values, which corresponded to the newly formed bone. The mean of the peak related to the newly formed bone shifted to higher values of linear attenuation coefficient as the implantation time increased. This effect can be explained by a progressive increase in the degree of mineral concentration of bone as a function of implantation time.

In another work [30], by exploiting the advantages of micro-CT associated with synchrotron radiation, Si-TCP (silicon-tricalcium phosphate) scaffolds were characterized and the 3D bone deposition into tissue engineering constructs *in vivo* at different implantation times evaluated. Analyses of the ceramic scaffolds were performed before and after 2, 4, and 6 months of implantation. The results indicated that there was an increment of the new bone thickness during implantation, while the thickness of the scaffold progressively decreased. Interestingly, the segmentation process showed a progressive alteration of the new bone and scaffold densities from the 2-month to the 4- and 6-month implants. As the implantation time increased, bone mineralization took place, thus making it denser. On the contrary, all Si-TCP scaffolds, that before implantation presented a homogeneous density, after cell seeding and implantation displayed locally segregated different densities. Through evaluation of the thickness of the scaffold walls a remarkable resorption of the biomaterial was determined especially in the 4- and 6-month implants.

Vasculature within scaffolds

Tissue engineering as a therapeutical approach to regenerate lost or diseased tissues or organs via delivery of cells, constructs and biomolecules to the appropriate site requires a functional vascular networks for adequate integration. It is generally accepted today that vascularization of cell engrafted matrices and scaffold is critical for the survival and proper function of tissue engineering constructs. Thus, a key issue in fabricating translatable regenerative tissue is the ability to generate a functional microvascular network within engineered constructs to provide oxygen and nutrients that facilitate growth, differentiation, and tissue functionality [31]. Oxygen and nutrient diffusion are effective within 200 μm of a vascular supply source. The development of a functional vasculature is particularly critical in respect to bone defects which can be extensive. Therefore, research using tissue engineering strategies has increasingly focused on angiogenesis into biomaterials.

Due to their low attenuation and small diameter, blood vessels are difficult to image in micro-CT. Radio-opaque contrast agents have enabled the visualization of microvasculature in tissues [32, 33]. However, none of these studies involved quantification of the vasculature or the imaging of newly formed vessels in tissue engineering constructs. Duvall *et al.* [34] used contrast enhanced micro-CT analysis to quantify morphologic parameters, including vessel volume, thickness, number, connectivity, and degree of anisotropy of a 3D vascular network. Briefly, the technique involves perfusion of a radiodense silicone rubber contrast agent, "Microfil", containing lead chromate and a curing agent through the vasculature immediately following euthanasia. The explanted samples were demineralised prior to scanning to allow segmentation of the vascular networks.

The development of a functional vasculature is particularly critical with respect to the augment, growth and repair of bone loss particularly in areas of trauma, degeneration and revision surgery. However, the initiation and development of a fully functional vascular network are critical for bioengineered bone to repair large osseous defects, whether the material is osteosynthetic (poly(D,L)-lactic acid, PLA) or natural bone allograft. For example, in impact bone grafting for revision surgery (a recognised technique to develop bone using morsellized allograft) a blood supply will be a significant distance away from the

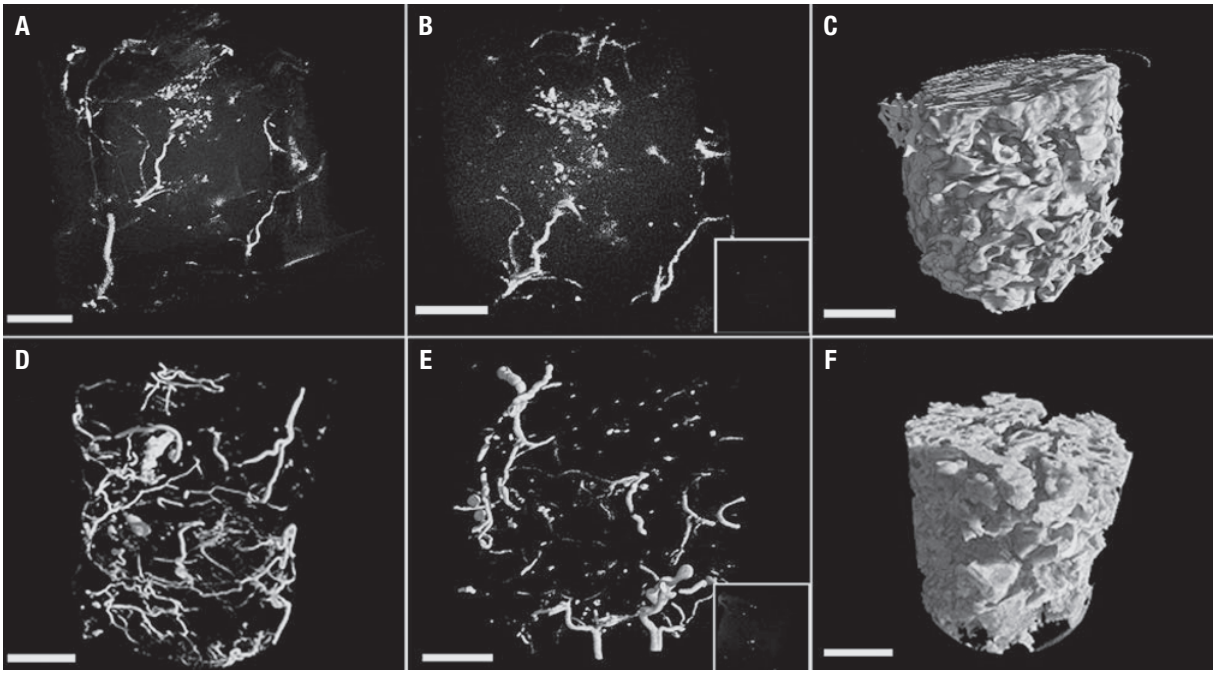

Fig. 5 | *3D micro-CT visualization of vessel networks. Micro-CT 3D reconstructions demonstrating new vessel formation outside (A) and inside (B) the impacted allograft/HBMSC capsules compared to allograft alone (B insert) and outside (E) the impacted PLA/HBMSC samples compared to PLA (E insert) alone. 3D reconstructions of the impacted scaffolds: (C) allograft, (F) PLA. Reproduced from Bolland* et al. *[36], with permission of Elsevier.*

central regions of the tissue. The proximity of this vascular supply will become critical when this technique is combined with mesenchymal stem cells to help regenerate the bone [35].

Bolland *et al.* [36] also used the "Microfil" technique to study angiogenesis in tissue engineering constructs combining human bone marrow stromal cells (HBMSC) with natural allograft and synthetic graft (PLA) implanted into the subcutis of immunosuppressed mice for a period of 28 days. Microfil was perfused through the anaesthetised mice by injecting it into the heart. Explanted and fixed samples were then scanned using a laboratory micro-CT scanner. *Figure 5* shows the 3D reconstruction of new vessel formation outside *(Figure 5A)* and inside *(Figure 5B)* the capsules in impacted allografts/HBMSC samples compared to allograft bone (B, insert). *Figure 5C* represents the 3D reconstruction of the impacted allograft scaffold. Similarly, new vessel formation was demonstrated outside *(Figure 5D)* and inside *(Figure 5E)* the capsules in impacted PLA/HBMS compared to PLA alone (E, insert). *Figure 5F* represents the 3D reconstruction of the impacted PLA scaffold. Quantification of several parameters within the scaffolds was achieved: total vessel volume; volume/volume of scaffold; vessel thickness; mean number of vessels per unit length and spacing between the vessels. The density (attenuation) of the silicone rubber was used to obtain the total vessel volume (total number of voxels corresponding to the silicone rubber) within each sample. Algorithms developed for bone structural material specifically for bone structural material parameters were applied to the grey scale values corresponding to the microfilling material. Vessel thickness (VTh) was determined by the ratio of vessel surface (VS) to the vessel volume (VV) and was calculated using the Cauchy-Crofton theorem *i.e.* VTh = 2/BS/BV, where BS is the bone surface and BV is the bone volume. The mean number of vessels per unit length (VN) was calculated using VN = (BV/TV)/VTh, where TV is the total number of vessels. The vessels spacing (VSp) between vessel structures was determined using VSp = 1/VN – VTh.

Schmidt *et al.* [37] used micro-CT for the evaluation of VEGF-induced vessel ingrowth into a porous polyurethane scaffold through comparison with analysis by CD31 immunohystochemistry. Micro-CT allowed quantitative vessel detection almost down to the capillary level across the whole length of the implant. The strength of micro-CT was almost apparent in the analysis of the expected increase in vascularization induced by VEG, qualitatively showing very clearly the marked increase in, and more importantly the distribution of, the induced vessel across the entire construct. A limitation of the micro-CT technique was the overestimation of average vessel size by 1.58 to 1.91 fold increase when compared to histologically assessed Microfil filled vessels. This is presumably due to a merging effect of vessels lying next to each other with an inter-vessels distance of less than 12 μm [38].

CONCLUSIONS

Micro-CT is a rather new technique but it has demonstrated various key advantages. Being a computational method, numerous parameters can be calculated and this depends on the computational capability of the software and hardcore. Furthermore, it is non destructive, hence samples remain intact for further analysis. Now, there is a shift emphasis from improving the imaging technique, to developing new and improved image analysis technique to get the most from the 3D images, as well as to monitor 3D cell response *in vitro* and bone and blood vessel ingrowth, including quality of blood vessels.

Conflict of interest statement

There are no potential conflicts of interest or any financial or personal relationships with other people or organizations that could inappropriately bias conduct and findings of this study.

Submitted on invitation.
Accepted on 19 December 2011.

References

1. Whang K, Healy KE, Elenz DR, Nam EK, Tsai DC, Thomas CH, Nuber GW, Glorieux FH, Travers R, Sprague SM. Engineering bone regeneration with bioabsorbable scaffolds with novel microarchitecture. *Tissue Eng* 1999;5(1):35-51. DOI: 10.1016/j.actbio.2008.02.029.
2. Cornell CN. Osteoconductive materials and their role as substitutes for autogenous bone grafts. *Orthop Clin North Am* 1999; 30(4):591-8.
3. Boyan BD, Lohmann CH, Romero J, Schwartz Z. Bone and cartilage tissue engineering. *Clin Plast Surg* 1999;26(4):629-45, ix. DOI: 10.1186/1746-160X-3-4
4. Zein I, Hutmacher DW, Tan KC, Teoh SH. Fused deposition modeling of novel scaffold architectures for tissue engineering applications. *Biomaterials* 2002;23(4):1169-85. DOI: 10.4028/www.scientific.net/JBBTE.6.57
5. Meinel L, Karageorgiou V, Fajardo R, Snyder B, Shinde-Patil V, Zichner L, Kaplan D, Langer R, Vunjak-Novakovic G. Bone tissue engineering using human mesenchymal stem cells: effects of scaffold material and medium flow. *Ann Biomed Eng* 2004;32(1):112-22. DOI: 10.1089/ten.tea.2009.0164
6. Kim BS, Mooney DJ. Development of biocompatible synthetic extracellular matrices for tissue engineering. *Trends Biotechnol* 1998;16(5):224-30. DOI: 10.1016/0167-7799(90)90139-O
7. Mooney DJ, Mazzoni CL, Breuer C, McNamara K, Hern D, Vacanti JP, Langer R. Stabilized polyglycolic acid fibre-based tubes for tissue engineering. *Biomaterials* 1996;17(2):115-24. DOI: 10.1016/0142- 9612(96)89774-2
8. Guldberg RE, Lin AS, Coleman R, Robertson G, Duvall C. Microcomputed tomography imaging of skeletal development and growth. *Birth Defects Res C Embryo Today* 2004; 72(3):250-9. Review. DOI: 10.1002/bdrc.20016
9. Guldberg RE, Ballock RT, Boyan BD, Duvall CL, Lin AS, Nagaraja S, Oest M, Phillips J, Porter BD, Robertson G, Taylor WR. Analyzing bone, blood vessels, and biomaterials with microcomputed tomography. *IEEE Eng Med Biol Mag* 2003;22(5):77-83.
10. Chappard C, Peyrin F, Bonnassie A, Lemineur G, Brunet-Imbault B, Lespessailles E, Benhamou CL. Subchondral bone micro-architectural alterations in osteoarthritis: a synchrotron micro-computed tomography study. *Osteoarthritis Cartilage* 2006;14(3):215-23.
11. Weiss P, Obadia L, Magne D, Bourges X, Rau C, Weitkamp T, Khairoun I, Bouler JM, Chappard D, Gauthier O, Daculsi G. Synchrotron X-ray microtomography (on a micron scale) provides three-dimensional imaging representation of bone ingrowth in calcium phosphate biomaterials. *Biomaterials* 2003;24(25):4591-601. DOI: 10.1016/S0142-9612(03)00335-1
12. Ortiz MC, García-Sanz A, Bentley MD, Fortepiani LA, García-Estañ J, Ritman EL, Romero JC, Juncos LA. Microcomputed tomography of kidneys following chronic bile duct ligation. *Kidney Int* 2000;58(4):1632-40. DOI: 10.1046/j.1523-1755.2000. 00324.x
13. Verna C, Dalstra M, Wikesjö UM, Trombelli L; Carles Bosch. Healing patterns in calvarial bone defects following guided bone regeneration in rats. A micro-CT scan analysis. *J Clin Periodontol* 2002;29(9):865-70. DOI: 10.1034/j.1600-051X.2002.290912.x
14. Bentley MD, Ortiz MC, Ritman EL, Romero JC. The use of microcomputed tomography to study microvasculature in small rodents. *Am J Physiol Regul Integr Comp Physiol* 2002;282(5):R1267-79. DOI: 10.1186/2040-2384-2-7
15. Sun W, Starly B, Darling A, Gomez C. Computer-aided tissue engineering: application to biomimetic modelling and design of tissue scaffolds. *Biotechnol Appl Biochem* 2004;39(Pt 1):49-58. DOI: 10.1055/s-2005-919717
16. Meinel L, Karageorgiou V, Fajardo R, Snyder B, Shinde-Patil V, Zichner L, Kaplan D, Langer R, Vunjak-Novakovic G. Bone tissue engineering using human mesenchymal stem cells: effects of scaffold material and medium flow. *Ann Biomed Eng* 2004;32(1):112-22. DOI: 10.1089/ten.tea.2009.0164
17. Duvall CL, Taylor WR, Weiss D, Guldberg RE. Quantitative microcomputed tomography analysis of collateral vessel development after ischemic injury. *Am J Physiol Heart Circ Physiol* 2004;287(1):H302-10. DOI: 10.1152/ajpheart.00199.2009
18. Verna C, Dalstra M, Wikesjö UM, Trombelli L; Carles Bosch. Healing patterns in calvarial bone defects following guided bone regeneration in rats. A micro-CT scan analysis. *J Clin Periodontol* 2002;29(9):865-70. DOI: 10.1034/j.1600-051X.2002.290912.x
19. X-ray computed microtomography (microCT) using synchrotron radiation (SR). Bonse U, Busch F. *Prog Biophys Mol Biol* 1996;65(1-2):133-69. DOI: 10.1016/j.bone.2010.08.023
20. Wang G, Vannier MW, Skinner MW, Cavalcanti MG, Harding GW. Spiral CT image deblurring for cochlear implantation. *IEEE Trans Med Imaging* 1998;17(2):251-62. DOI: 10.1016/S0079-6107(96)00011-9
21. Wang G, Schweiger G, Vannier MW. An iterative algorithm for X-ray CT fluoroscopy. *IEEE Trans Med Imaging* 1998; 17(5):853-6.
22. Barbetta A, Barigelli E, Dentini M. Porous alginate hydrogels: synthetic methods for tailoring the porous texture. *Biomacromolecules* 2009;10(8):2328-37.
23. Barbetta A, Gumiero A, Pecci R, Bedini R, Dentini M. Gas-in-liquid foam templating as a method for the production of highly porous scaffolds. *Biomacromolecules* 2009; 10(12):3188-92.
24. Barbetta A, Rizzitelli G, Bedini R, Pecci R, Dentini M. Porous gelatin hydrogels by gas-in-liquid foam templating. *Soft Matter* 2010;6:1785-92.
25. Hedberg EL, Kroese-Deutman HC, Shih CK, Lemoine JJ, Liebschner MA, Miller MJ, Yasko AW, Crowther RS, Carney DH, Mikos AG, Jansen JA. Methods: a comparative analysis of radiography, microcomputed tomography, and histology for bone tissue engineering. *Tissue Eng* 2005;11(9-10):1356-67. DOI: 10.1089/ten.2005.11.1356

26. Weiss P, Obadia L, Magne D, Bourges X, Rau C, Weitkamp T, Khairoun I, Bouler JM, Chappard D, Gauthier O, Daculsi G. Synchrotron X-ray microtomography (on a micron scale) provides three-dimensional imaging representation of bone ingrowth in calcium phosphate biomaterials. *Biomaterials* 2003;24(25):4591-601. DOI: 10.1016/S0142-9612(03)00335-1
27. Cherry SR. *In vivo* molecular and genomic imaging: new challenges for imaging physics. *Phys Med Biol* 2004;49(3): R13-48. Review. doi:10.1088/0031-9155/49/3/R01.
28. Mastrogiacomo M, Komlev VS, Hausard M, Peyrin F, Turquier F, Casari S, Cedola A, Rustichelli F, Cancedda R. Synchrotron radiation microtomography of bone engineered from bone marrow stromal cells. *Tissue Eng* 2004;10(11-12):1767-74.
29. Komlev VS, Peyrin F, Mastrogiacomo M, Cedola A, Papadimitropoulos A, Rustichelli F, Cancedda R. Kinetics of *in vivo* bone deposition by bone marrow stromal cells into porous calcium phosphate scaffolds: an X-ray computed microtomography study. *Tissue Eng* 2006;12(12):3449-58.
30. Papadimitropoulos A, Mastrogiacomo M, Peyrin F, Molinari E, Komlev VS, Rustichelli F, Cancedda R. Kinetics of *in vivo* bone deposition by bone marrow stromal cells within a resorbable porous calcium phosphate scaffold: an X-ray computed microtomography study. *Biotechnol Bioeng* 2007;98(1):271-81.
31. Brey EM, King TW, Johnston C, McIntire LV, Reece GP, Patrick CW Jr. A technique for quantitative three-dimensional analysis of microvascular structure. *Microvasc Res* 2002;63(3): 279-94. doi: 10.1371/journal.pone.0028290
32. Toyota E, Fujimoto K, Ogasawara Y, Kajita T, Shigeto F, Matsumoto T, Goto M, Kajiya F. Dynamic changes in three-dimensional architecture and vascular volume of transmural coronary microvasculature between diastolic- and systolic-arrested rat hearts. *Circulation* 2002;105(5):621-6. DOI: 10.1161/hc0502.102964
33. Plouraboue F, Cloetens P, Fonta C, Steyer A, Lauwers F, Marc-Vergnes JP. X-ray high-resolution vascular network imaging. *J Microsc* 2004;215(Pt 2):139-48. DOI: 10.1111/j.0022-2720.2004.01362.x
34. Duvall CL, Taylor WR, Weiss D, Guldberg RE. Quantitative microcomputed tomography analysis of collateral vessel development after ischemic injury. *Am J Physiol Heart Circ Physiol* 2004;287(1):H302-10. doi: 10.1152/ajpheart.00199.2009
35. Bolland BJ, Tilley S, New AM, Dunlop DG, Oreffo RO. Adult mesenchymal stem cells and impaction grafting: a new clinical paradigm shift. *Expert Rev Med Devices* 2007;4(3):393-404. Review. doi:10.1586/17434440.4.3.393
36. Bolland BJ, Kanczler JM, Dunlop DG, Oreffo RO. Development of *in vivo* microCT evaluation of neovascularisation in tissue engineered bone constructs. *Bone* 2008; 43(1):195-202. DOI: 10.1016/j.bone.2008.02.013
37. Schmidt C, Bezuidenhout D, Beck M, Van der Merwe E, Zilla P, Davies N. Rapid three-dimensional quantification of VEGF-induced scaffold neovascularisation by microcomputed tomography. *Biomaterials* 2009;30(30):5959-68.
38. Ito M, Ejiri S, Jinnai H, Kono J, Ikeda S, Nishida A, Uesugi K, Yagi N, Tanaka M, Hayashi K. Bone structure and mineralization demonstrated using synchrotron radiation computed tomography (SR-CT) in animal models: preliminary findings. *J Bone Miner Metab* 2003;21(5):287-93 doi: 10.1111/j.1365-2818.2010.03381.x.